International Journal of u- and e- Service, Science and Technology
Vol.9, No. 6 (2016), pp.59-68
http://dx.doi.org/10.14257/ijunesst.2016.9.6.06

Input Seismic Motion Based on the Viscous-Spring Boundary: Analytical Solution and Numerical Simulation

Xue Zhicheng[1*], Pei Qiang[2], Wu Shuang[2] and Pan Changfeng[1]

[1]*School of Civil Engineering*
Heilongjiang Institute of Science and Technology Harbin, China
[2]*The R&D Center of the Civil Engineering Technolog*
Dalian University, Dalian, China
**xuezc0621@163.com*

Abstract

Practical geotechnical engineering problems are usually solved within an infinite half-space domain, and a finite domain is necessary to analyze the dynamic response of the medium by the finite element method (FEM). How to deal with the boundary is vital for obtaining accurate results in numerical simulation. This study obtains the analytical solution of input stress at the boundary based on the viscous-spring boundary and develops a procedure for the two-dimensional artificial viscous-spring boundary application in the seismic analysis. The analytical solution based on the viscous-spring boundary is verified using other three artificial boundaries. Furthermore, the simulation accuracy of the procedure is carried out by establishing a two-dimensional model for different element sizes and modified coefficients. The results show that the element size must be in a certain range to avoid the loss of main frequency of seismic motions. When the modified coefficient is less than the suggested value, obvious shifts appear on the calculation results. On the opposite, when the modified coefficient is greater than that, the result will fluctuate dramatically before convergence. All the above factors can lead to a distortion of simulation accuracy of artificial boundary model. Compared with the viscous boundary, viscous-spring boundary has higher simulation accuracy.

Keywords*: Soil-structure interaction; Viscous-spring boundary;Input seismic motion,Finite element method*

1. Introduction

Practical civil engineering problems are usually analyzed using the vibration and wave propagation in an elastic infinite half-space domain. These problems include such problems as the foundation vibration induced by dynamic machine, vibration induced by pile driving and road traffic, and the seismic wave transmission in various media, *etc*, which belong to the dynamic soil-structure interaction scope [1]. Considering infinite foundation simulation is the main research area in soil-structure interaction problem. FEM is an appropriate method for dynamic analysis, and a finite domain is usually used by cutting artificial boundaries, known as the near field. Then the structure and the near field are modeled using the finite element method. The effective and efficient application of the method for solving the dynamic soil-structure interaction problems may be challenged by the artificial boundaries due to its wave reflection and refraction problems or how large the field of a structure is considered.

The artificial boundaries can be classified into two types: (1) global artificial boundaries [2], which require the total boundary conditions, physical equations, and the radiation coditions near an infinite far field are satisfied for the travelling wave. Therefore, the accuracy can be assured for simulating the infinite foundation. However, the challenge of coupling time and space must be solved; and (2) local artificial boundary condition [3],

ISSN: 2005-4246 IJUNESST

which deals with the coupling of space and time, results in an efficient numerical procedure, with the above conditions not strictly satisfied. These local boundary conditions include the paraxial approximation boundary [4], the artificial transmitting boundary [5] and the viscous spring boundary[6]. Among these local artificial boundaries, the viscous-spring boundary attracted the researchers due to the advantages of simple modeling, clear physical significance, and convenient application in finite element method. This study investigates the modified coefficient and element size effects on the simulation accuracy of the viscous-spring boundary [7-9].

2. Governing Equations

Lysmer and Kuhlemeyer proposed the viscous boundary in 1969 by considering the propagation of a harmonic wave[10]. The boundary takes the energy absorption into account while ignores the simulation of the elastic restoring force in the semi-infinite space. As is noticed for this boundary, it may have stability problem when dealing with low frequency dynamic loads. The obvious numerical shifting may appear in simulation. To modify the weakness of the viscous boundary, Deeks, Liu and Du developed plain strain equations for axisymmetric shear and dilation waves based on an approximation of the form of the outward traveling waves. The main idea of the method is to regard the stress as the function of the corresponding displacement and the velocity thus the governing equations are as follows:

$$\sigma_{mj}(t) = -K_{mj}u_{mj}(t) - C_{mj}\dot{u}_{mj}(t) \tag{1}$$

Where the subscript *m* denotes the serial number of the node in the artificial boundary; subscript $j = x, y, z$ are the components in the x, y and z direction; t is the time; σ_{mj}, u_{mj} and $\dot{u}_{mj}$ represent the stress, displacement and velocity of node *m* in the *x* direction, and K_{mj} and C_{mj} represent the elastic and viscous parameters of node *m* in the *x* direction.

Consider the boundary element is placed at the node *M*, and then the boundary parameters can be calculated with the following Equations (2) and (3):

$$K_{MN} = \alpha_N G/R \cdot A, \quad C_{MN} = \rho C_P A \tag{2}$$

$$K_{MT} = \alpha_T G/R \cdot A, \quad C_{MT} = \rho C_S A \tag{3}$$

Where K_{MN} and K_{MT} denote the spring stiffness in the normal and tangential directions, respectively; C_{MN} and C_{MT} denote the damping coefficients in the normal and tangential directions, respectively; R denotes the distance between the earthquake source and the node; A is the equivalent area; C_P and C_S denote the transmitting velocity of the p wave and s wave in the soil; α_N and α_T denote the modified viscous-spring ity coefficients in the normal and tangential directions at the artificial boundary.

3. Analytical Solutions of Input Seismic Motion

For soil-structure interaction problems, the method to deal with the earthquake motion is very important to assure the calculation accuracy and reliability after selecting the appropriate boundary condition. Liu *et al.*, [11] regarded the input of the earthquake motion as the wave source problem. They replaced the input earthquake motion at the boundary nodes with the equivalent stress, making it possible to input earthquake motion in the time history analysis in the finite element model when dealing with the seismic problems.

Consider the force condition of the node at the artificial boundary; the force analysis is configured in Figure 1. The stress at the node is expressed as Equation (4):

$$F_B(t) = f_B(t) + \sigma_B(t) \tag{4}$$

Where F_B represents the applied stress at the node; f_B represents the stress at the viscous-spring boundary; σ_B represents stress in the non-cutting continuous media at the corresponding node.

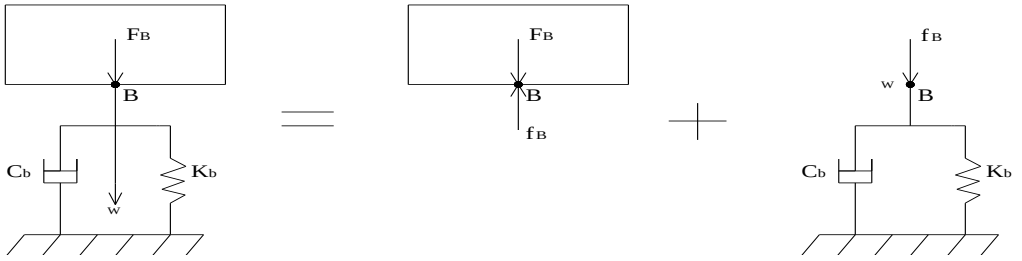

Figure 1. Schematic Diagram of the Force Analysis of the Node for the Viscous-Spring Boundary

3.1. Input Method of the Bottom Boundary Node

Assume the following condition, if the *p* wave originates from the bottom to the top, the tangential stresses and normal direction can be determined by the following Equations (5) and (6):

$$F_T^B = 0 \tag{5}$$

$$F_N^B = K_N u_r + C_N \dot{u}_r + \rho c_p \dot{u}_r \tag{6}$$

Where K_N, C_N and ρ represent the coefficient of the normal elastic element, the coefficient and the media density at the viscous-spring boundary bottom.

Likewise, the input tangential stress and the normal stress can be determined by the following Equations (7) and (8), if *s* wave originates from the bottom to the top:

$$F_T^B = K_T u_r + C_T \dot{u}_r + \rho c_s \dot{u}_r \tag{7}$$

$$F_N^B = 0 \tag{8}$$

Where K_T and C_T represent the coefficient of the tangential elastic element and the coefficient of the tangential viscous element at the bottom of the viscous-spring boundary.

Consider the reflection of the free surface wave, the stress at the node of the viscous-spring boundary is expressed as follows:

$$F_S^B(t) = F^B(t) + F^B(t - \frac{2h}{c}) \tag{9}$$

Where $F_S^B(t)$ denotes the actual input stress at the node of viscous-spring boundary at *t* time; *h* is the total height of the model and *c* is the transmitting velocity of the earthquake motion in the media.

3.2. Input Method of the Lateral Boundary Node

Assume the following condition, if *p* wave originates from the bottom to the top, the tangential and normal stresses at the lateral node can be determined by the following Equations (10) and (11):

$$F_T^S = K_T u_f + C_T \dot{u}_f \tag{10}$$

$$F_N^S = \frac{\lambda}{\lambda + 2G} \rho c_p \dot{u}_f \tag{11}$$

Where K_T and C_T are the stiffness coefficient of the tangential elastic element and the damping coefficient of the tangential viscous element at the lateral viscous-spring boundary.

If *s* wave transmits from the bottom to the top, the normal input stress at the lateral boundary is expressed as the follows:

$$F_N^S = K_N u_f + C_N \dot{u}_f \tag{12}$$

$$F_T^{S左} = \rho c_s \dot{u}_f \tag{13}$$

$$F_T^{S右} = -\rho c_s \dot{u}_f \tag{14}$$

Where K_N and C_N denote the coefficients of the normal elastic element and viscous element at the lateral boundary.

Consider the reflection of the wave at the free surface and the phase difference between the lateral boundary node and the bottom node, the actual input stress at the lateral boundary node is as follows:

$$F_S^S(t) = F^S(t - \frac{l}{c}) + F^S(t - \frac{2h - l}{c}) \tag{15}$$

Where $F_S^S(t)$ denotes the actual input stress at the node of lateral viscous-spring boundary at t time; *h* is the total height of the model and *l* is the distance between the lateral boundary node and the bottom boundary node.

The above equations are the stresses at the node, which should be replaced with the equivalent stresses when conducting earthquake input motion using the finite element method. Furthermore, all the coefficients of the elastic element and viscous element and the modified coefficients relate to the soil layer parameters. Therefore, the above coefficients, soil density and earthquake wave velocity of the node at various heights of the lateral boundary should be selected based on the soil layer parameters.

4. Accuracy of the Viscous-Spring Boundary

The two dimensional homogeneous elastic half space models were established to evaluate the accuracy of the viscous-spring boundary by comparing viscous and viscous-spring boundaries, respectively. The calculation domain is $2m \times 2m$, shown in Figure 2. The plain strain element is selected with the element size of $\Delta x = \Delta y = 0.1m$. The input wave is the distributed load $F(t)$ applying on the elastic half space surface along y axis. The distributed load is expressed in Equation (16) and the calculation time $t = 10s$. The

accuracy is evaluated by comparing the vertical displacements of point A(0,1.5) and point B(0,1) in Figure 2.

$$F(t) = \begin{cases} t, & 0 \le t \le 0.5 \\ 1-t, & 0.5 \le t \le 1 \\ 0, & t \rangle 1 \end{cases} \tag{16}$$

The modified coefficients of α_T and α_N are 0.5 and 1.0, respectively. The media parameters are listed in Table 1.

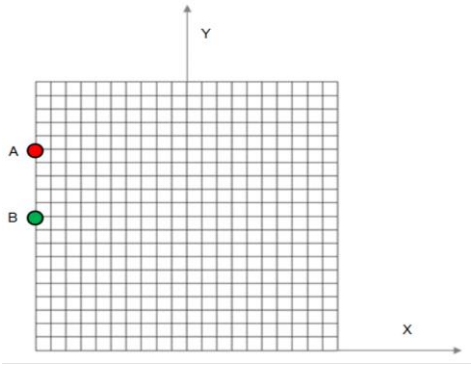

Figure 2. Two Dimensional Calculation Model for the Homogeneous Elastic Half Space

Table 1. Media Parameters

Media parameters	Values
Shear modulus	$G=1$
Poisson's ratio	$\upsilon=0.25$
Density	$\rho=1$
Velocity of S wave	$C_S=1$
Velocity of P wave	$C_P=\sqrt{3}$

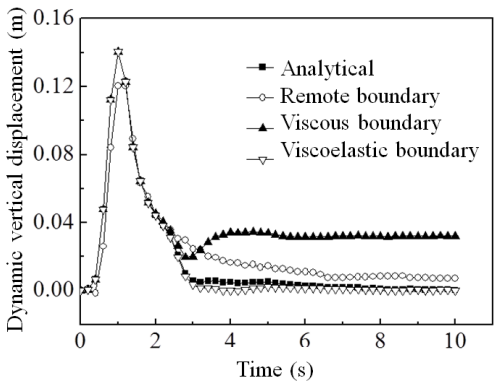

(a) Point A

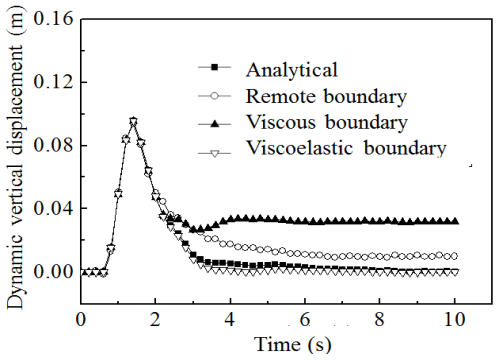

(b) Point B

Figure 3. Time Histories of Dynamic Displacements at Points A and B for Different Boundary Conditions

Figure 3 shows the time histories of the displacements at points A and B. It is clear that the displacements shifts for the viscous boundary while tends to converge to the initial equilibrium position for the viscous-spring boundary. Additionally, the dynamic displacements calculated using viscous-spring boundary agree well with the analytical solution and those calculated using the remote boundary. These results indicate the numerical model using the viscous-spring boundary well simulates the radiation damping of the soil with the favorable accuracy.

Table 2. The Modified Coefficients α_N and α_T

Parameter	Value range	Suggested coefficient
α_N	0.8~1.2	2/2
α_T	0.35~0.65	1/2

5. Influential Factors

Although the viscous-spring boundary has the favorable simulation capacity and excellent dynamic stability, it is still influenced by various factors in numerical simulation. This study investigates the modified coefficients and element size effects on the results.

5.1. Modified Coefficients

The simulation accuracy relates to the modified coefficients α_N and α_T, shown in Equations (2) and (3). Literature [11] suggested the value ranges of α_N and α_T when dealing with two dimensional problems, which are verified in literatures [12-13].

Figure 4 shows the time histories of dynamic displacements of points A and B for different modified parameters α_N and α_T. It can be seen from Figure 4 that when α_N and α_T are less than the suggested values, obvious shifts appear at the time histories of the dynamic displacements. On the contrary, distinct fluctuations appear at the time histories of the dynamic displacements before convergence. It is concluded that selecting the reasonable values of the modified parameters is greatly significant to improve the simulation accuracy using the viscous-spring boundary.

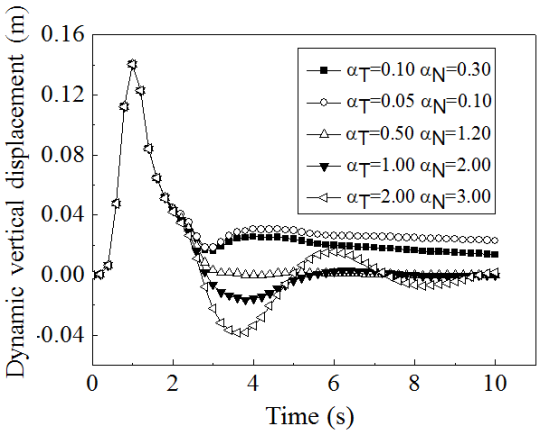

(a) Point A

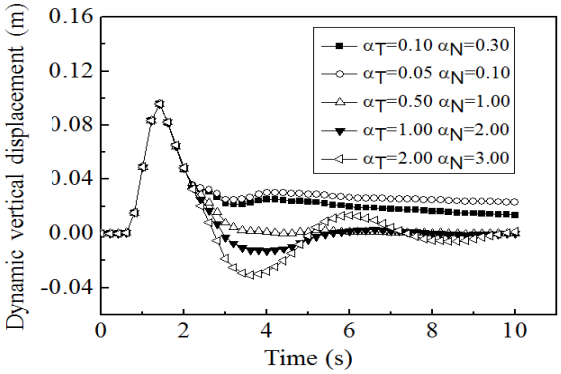

(b) Point B

Figure 4. Time Histories of Dynamic Displacements at Points A and B for Different Modified Parameters

5.2. Element Size

In numerical simulation using the finite element method solving the wave propagation problems, the element size should be as small as possible to assure no loss of the main energy during wave propagating in the discrete finite element grids. However, the finer the element grids, the longer the calculation process will require. Therefore, it is important to optimize the element size to improve the simulation accuracy and save time.

The element size usually depends on the wavelength of the harmonic component of the structure, which is determined by $\boldsymbol{d}/\lambda$. Lysmer *et al.*[14] proposed the element size was in the range of $\boldsymbol{d}/\lambda \le 1/12$. Liao and Liu[15] considered the reliable simulation results were obtained only if $\boldsymbol{d} \approx (1/10 \sim 1/8)\lambda$.

The element size *d* was adopted in the range between $1/10\lambda$ and $1/8\lambda$ in this study. Figure 5 shows the time histories of dynamic displacements at points A and B for different element sizes. It is shown that the dynamic results will fluctuate if the element size is not within the adopted range while remains stable if it is in the selected range. Therefore the adopted element size should be in the range between $1/10\lambda$ and $1/8\lambda$ to make input earthquake motion lose no energy.

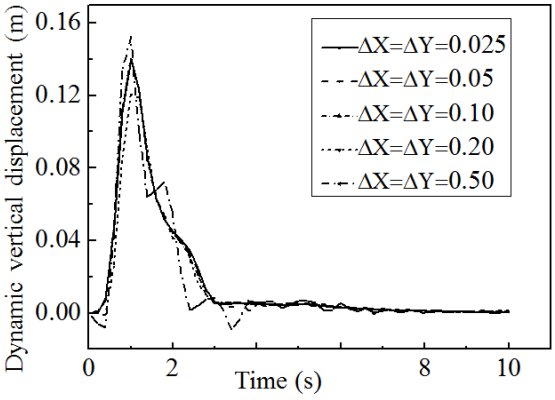

(a) Point A

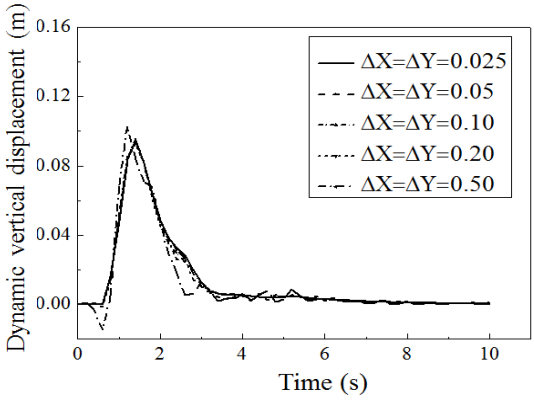

(b) Point B

Figure 5. Time Histories of Dynamic Displacements at Points A and B for Different Element Sizes

6. Conclusion

This study obtained the analytical solution of input stress at the boundary based on the viscous-spring boundary and the solution was applied in the finite element method using ANSYS. Then, the analytical solution was verified using the plain strain problem and the influential factors affecting the simulation accuracy was investigated. This indicates the numerical model can be used in the engineering problems.

Acknowledgments

"*" is corresponding author, the paper is supported by Natural Science Foundation of China (contracts no: 51478168, 51378085,11572113) and Technology Research Program Foundation of Heilongjiang Province Education Departmen (contracts no: 12541694) and Project supported by the Maor International Joint Research Program of China (contracts no: 2013DFA71120)

References

[1] F. Zhi, "Dynamic response and artificial boundary analysis in soil structure interaction system", Chinese Quarterly of Mechanics, vol. 30, no. 3, **(2009)**, pp. 475-480.
[2] L. Zhenpeng, "Introduction to wave motion theories in engineering", Science Press, Beijing, **(2002)**.
[3] E. Kausel, "Local Transmitting boundaries", Journal of Engineering Mechanics, vol. 114, no. 6, **(1988)**, pp. 1011-1027.
[4] R. Clayton and B. Engquist, "Absorbing boundary conditions for acoustic and elastic wave equations", Journal of Bull. Seism. Soc. Amer., vol. 76 , no. 2, **(1977)**, pp. 1529-1540.

[5] L. Zhenpen, H. Kongliang and Y. Baibo, "Transient wave transmitting boundary", Journal Science in China(Ser. E), vol. 26, no. 6, **(1984)**, pp. 50-56.
[6] A. J. Deeks and M. F. Randolph, "Axisymmetric time-domain transmitting boundaries", Journal of Engineering Mechanics, ASCE, vol. 120, no. 1, **(1994)**, pp. 25-42.
[7] C. G. Zhou, "Research on the mechanism of seismic wave input about high rockfill dam", Dalian University of Technology, **(2009)**.
[8] Z. Mi, "Study on the viscous-spring boundary and the transmitting boundary", Beijing University of Technology, **(2004)**.
[9] J. Tong and Z. Xin, "Dynamic analysis of elastic half space problems by using FEM with viscous boundary element", Chinese Quarterly of Mechanics, vol. 25, no. 4, **(2004)**, pp. 535-540.
[10] J Lysmer and R. L. Kuhlemeyer, "Finite dynamic model for infinite media", Journal of the Engineering Mechanics Division, ASCE, vol. 95, no. 1, **(1969)**, pp. 859-877.
[11] L. Jingbo, D. Yixin and Y. Qiushi, "Visco-elastic and the ground motion input implement in the general finite element softwar", Journal of Disaster Prevention and Mitigation Engineering, **(2007)**, no. 27, pp. 37-42.
[12] L. C. Qiu, L. Hua and J. Feng, "Time-domain finite-element analysis of two dimensional seismic soil-structure interactions", Journal of Engineering mechanics, vol. 23, no. 9, **(2006)**, pp. 114-119.
[13] L. Jingbo, G. Yin and D. Yixin, "Consistent viscous-spring artificial boundaries and viscous-spring boundary elements", Chinese Journal of Geotechnical Engineering, vol. 28, no. 9, **(2006)**, pp. 1070-1075.
[14] J. Lysmer and R. L. Kuhlemeyer, "Finite dynamic model for infinite media", Journal of Engineering Mechanics, ASCE, (EM4), no. 95, **(1969)**, pp. 759-877.
[15] L. Zhenpeng and L. Jingbo, "Elastic wave motion in discrete grids", Journal of Earthquake Engineering and Engineering Vibration, vol. 6, no. 2, **(1986)**, pp. 1-16.